Journal of Applied Physics

RESEARCH ARTICLE | MAY 14 2024

Hydrogen passivation of acceptor defects in delafossite $CuMO_2$ (M = Al, Ga, In): Insights for enhanced p-type conductivity

Aroon Ananchuensook ; Intuon Chatratin ; Anderson Janotti ; Teeraphat Watcharatharapong ; Jiraroj T-Thienprasert ; Adisak Boonchun ; Sirichok Jungthawan ; Pakpoom Reunchan

J. Appl. Phys. 135, 185705 (2024)
https://doi.org/10.1063/5.0201483

AIP Publishing

Journal of Applied Physics ARTICLE pubs.aip.org/aip/jap

Hydrogen passivation of acceptor defects in delafossite $CuMO_2$ (M = Al, Ga, In): Insights for enhanced p-type conductivity

Cite as: J. Appl. Phys. **135**, 185705 (2024); doi: 10.1063/5.0201483
Submitted: 30 January 2024 · Accepted: 30 April 2024 ·
Published Online: 14 May 2024

Aroon Ananchuensook,[1] Intuon Chatratin,[2] Anderson Janotti,[2] Teeraphat Watcharatharapong,[1] Jiraroj T-Thienprasert,[1] Adisak Boonchun,[1] Sirichok Jungthawan,[3] and Pakpoom Reunchan[1,a)]

AFFILIATIONS

[1]Department of Physics, Faculty of Science, Kasetsart University, Bangkok 10900, Thailand
[2]Department of Materials Science and Engineering, University of Delaware, Newark, Delaware 19716, USA
[3]School of Physics, Institute of Science, Suranaree University of Technology, Nakhon Ratchasima 30000, Thailand

Note: This paper is part of the special topic, Defects in Semiconductors 2024.
[a)]**Author to whom correspondence should be addressed:** pakpoom.r@ku.ac.th

ABSTRACT

Transparent conducting oxides with p-type conductivity hold immense potential for various electronic applications. The role of native point defects in delafossite $CuMO_2$ (M = Al, Ga, In) as the source of p-type conductivity has been widely acknowledged. However, understanding the primary defects governing the electrical properties and devising strategies for improvement remains a critical challenge. In this study, we employ range-separated hybrid density functional calculations to elucidate the impact of acceptor defects and their interactions with hydrogen on electrical conductivity. Our findings demonstrate that hydrogen plays a pivotal role in controlling p-type conductivity in these oxides. Our investigation reveals that the interactions between hydrogen interstitial H_i and copper vacancy V_{Cu} lead to the formation of stable complexes that are electrically inactive. Considerable binding energies are observed for H_i–V_{Cu} complexes, indicating that they are highly bound complexes with low formation energy and, thus, high concentrations under both O-rich and O-poor conditions. A second hydrogen can be bound to V_{Cu} to form $2H_i$–V_{Cu} complexes, which are thermodynamically stable and function as a single donor. Furthermore, hydrogen can bind with the antisite acceptor defects, Cu_M, forming H_i–Cu_M complexes. However, the lower binding energies associated with these complexes suggest likely dissociation into isolated H_i and Cu_M at relatively low temperatures. By shedding light on the strong influence of hydrogen passivation of acceptor defects, this study offers valuable insights into p-type conductivity in delafossite $CuMO_2$.

I. INTRODUCTION

Transparent conductive oxides (TCOs) are materials that possess the unique qualities of being both electrically conductive and transparent to visible light.[1] These materials have become increasingly important in developing advanced technologies, such as transparent electrodes for touch screens, displays, and photovoltaic cells. In optoelectronics, Sn-doped In_2O_3, ZnO, and SnO_2 are commonly employed as prototypical n-type TCOs, offering reliable and effective performance and are already commercialized.[2] The conduction band of these TCOs is composed of cation-*s* orbital, leading to low electron effective mass and high n-type conductivity.[2–4]

On the other hand, achieving p-type conductivity in these oxides is more challenging as their valence bands are mainly composed of O-2*p* orbitals, resulting in low dispersions (high effective masses) and lie deep in the energy scale with respect to vacuum. An approach to overcome this drawback has been proposed based on the electronic structure of n-type TCOs. The design principle is to modulate the O-2*p* bands, which are highly localized due to the high electronegativity of the O atoms.[5,6] It has been proposed to

utilize the metal d orbitals with energy levels comparable to those of O-2p orbitals. Cu^+, with electronic configuration $3d^{10}4s^0$, has been adopted as a promising candidate because the completely filled Cu 3d states lie just above the O-2p bands.[7,8] Spatial overlapping between Cu-3d and O-2p is expected to give a more dispersive valence band, raising the valence band position and decreasing the hole effective mass. This ends up being beneficial for p-type doping and hole transport. In addition, it requires maximizing the distance between Cu atoms to avoid interband d–d transitions that cause the coloration and lower the conduction band.[5] Kawazoe and Hosono have pioneered this approach, leading the discoveries of several p-type TCOs, including the delafossites $CuMO_2$ (M = Al, Ga, In). Hole conductivity, yet relatively low, was observed in the as-grown thin films of $CuAlO_2$[8] and $CuGaO_2$,[9] while $CuAlO_2$ exhibited bipolarity in electrical conduction upon external doping.[10] Several experimental[11–18] and theoretical studies[19–24] were conducted following these discoveries to identify the source of p-type conductivity and to improve the performance of these and other potential p-type oxides. It has been suggested that copper vacancies (V_{Cu}) and copper antisites (Cu_M) are the dominant defects causing the observed p-type conductivity in $CuMO_2$.[18,22,23]

Hydrogen has been known to affect the electrical properties of many metal oxides, particularly n-type TCOs. It was shown by theory and experiments that hydrogen impurity behaves as a shallow donor in ZnO,[25,26] In_2O_3,[27] SnO_2,[28,29] and Ga_2O_3.[30] Hydrogen interstitial (H_i) and substitution on the O site (H_O) were identified as shallow donors in these oxides.[26] In n-type materials, the negatively charged cation vacancies were shown to have low formation energy, forming in significant concentration. Hydrogen interstitial (H_i) has been shown to bind strongly to cation vacancies in n-type ZnO,[31] SnO_2, In_2O_3, and Ga_2O_3.[32] These complexes are very stable up to very high temperatures. The passivation of the negatively charged cation vacancies was suggested to reduce carrier scattering centers and, thus, enhance electron mobility.[32] It has been concluded that the hydrogenation of cation vacancies is very likely to occur in TCOs in general. Recently, the hydrogenation of cation vacancies in $SrTiO_3$[33] and Ga_2O_3[34] has been reported by theory and experiments. In contrast to the vast number of studies on hydrogen impurities in n-type metal oxides, only a few studies have been conducted on hydrogen impurities in p-type metal oxides. As far as we know, only a few theoretical studies based on the hybrid functional calculations have been reported for the behavior of hydrogen impurities and the passivation of the acceptor defects in Cu_2O.[35,36] It was revealed that H_i strongly binds with V_{Cu}, resulting in a stable H_i–V_{Cu} complex, which likely suppresses p-type conductivity.[35] Some isolated H_i configurations were studied in $CuAlO_2$ and $CuInO_2$.[37] It is, therefore, imperative to uncover the role of hydrogen in these delafossite metal oxides as it may play an important role in controlling their p-type conductivity.

The present article reports an investigation of the interaction between hydrogen and acceptor defects in delafossite $CuMO_2$ (M = Al, Ga, In) using range-separated hybrid density-functional calculations proposed by Heyd, Scuseria, and Ernzerhof (HSE). First, we investigate the energetics of hydrogen impurities in delafossites, taking $CuGaO_2$ as an example, and identify the lowest energy positively charged hydrogen impurity, found in the form of H_i, where H bonds to an O atom. The positively charged H_i forms a stable complex with the negatively charged V_{Cu}, resulting in effective passivation. Besides, we find that a second hydrogen can enter H_i–V_{Cu} to form $2H_i$–V_{Cu} complexes, which are thermodynamically stable and function as single donors. Finally, hydrogen can bind with the antisite acceptor defects, Cu_M, forming H_i–Cu_M complexes. The binding energies of these complexes are calculated and found to be sizable for the H_i–V_{Cu} complexes. In light of these results, we discuss the effects of hydrogen on hindering p-type conductivity and strategies to recover the $CuMO_2$-based device performance by post-annealing to remove hydrogen.

II. COMPUTATIONAL METHOD

Our calculations were based on the generalized Kohn–Sham theory[44] with the HSE hybrid functional,[45,46] as implemented in the VASP code.[47,48] Cu $3d^{10}4s^1$, Al $3s^23p^1$, Ga $4s^24p^1$, In $5s^25p^1$, O $2s^22p^4$ and the H $1s^1$ were treated as valence electrons within the projector augmented-wave method.[49,50] We employed a cutoff of 400 eV for the plane wave basis set. The fraction of Hartee–Fock (HF) exchange was set to 25% for all oxides with a screening length of 10 Å. This standard fraction yields bandgaps that agree with the experimental values, as listed in Table I. The periodic boundary conditions with the supercell approach were employed for the defect calculations. Effects of spin polarization are included. Symmetry-breaking distortions were considered for all cases. To study point native defects and the H impurity, we used a 108-atom supercell created by $3 \times 3 \times 1$ repetition of a 12-atom conventional cell of $CuMO_2$. A $(\frac{1}{4}, \frac{1}{4}, \frac{1}{4})$ special k point was used for the integrations over the Brillouin Zone. Test calculations show that using a denser mesh of special k point changes formation energies and transition levels by less than 0.15 eV. The lattice parameters are kept fixed during the structural relaxations, and the atoms are allowed to relax until the residual forces are less than 0.02 eV/Å. The defect formation energies can be used to derive defect concentrations under thermodynamic equilibrium, stability of different charge states, and related electronic transition levels. Determining the formation energies is thus essential to characterizing the defects and their energetics. Using, for example, the antisite Cu_M, where the Cu atom is replaced by an M atom, in charge state q, the

TABLE I. Calculated basic properties of $CuMO_2$, including lattice parameters, direct (E_g^{dir}) and indirect band gaps (E_g^{indir}), and formation enthalpy (ΔH_f). ΔH_f is estimated using Hess's law as described in the text. Available experimental values for lattice parameters,[38–40] bandgaps,[40–42] and ΔH_f[43] are also listed.

	$CuAlO_2$		$CuGaO_2$		$CuInO_2$	
	Calc.	Expt.	Calc.	Expt.	Calc.	Expt.
a(Å)	2.86	2.86	2.98	2.98	3.33	3.29
c(Å)	16.93	16.95	17.21	17.17	17.43	17.39
E_g^{dir} (eV)	5.27	3.53	3.79	3.75	2.54	4.45
E_g^{indir} (eV)	3.50	2.99	2.40	2.55	1.59	1.44
ΔH_f (eV)	−8.93	−9.50	−5.98	−6.44	−5.05	−5.60

TABLE II. Chemical potentials ($\tilde{\mu}_{Cu}$, $\tilde{\mu}_M$, and $\tilde{\mu}_O$) corresponding to $CuMO_2$ in O-rich and O-poor limits, expressed in eV.

	$CuAlO_2$	$CuGaO_2$	$CuInO_2$
O-rich	(−0.40, −6.47, −1.05)	(−0.49, −3.65, −0.92)	(−0.21, −2.37, −1.23)
O-poor	(0, −5.28, −1.84)	(0, −2.17, −1.90)	(0, −1.73, −1.66)

formation energy is defined as

$$E^f\left(Cu_M^q\right) = E_{tot}\left(Cu_M^q\right) - E_{tot}(CuMO_2) + \mu_M - \mu_{Cu} + q(\varepsilon_F + E_v) + \Delta^q, \quad (1)$$

where $E_{tot}\left(Cu_M^q\right)$ is the total energy of the supercell containing the antisite Cu_M in charge state q and $E_{tot}(CuMO_2)$ is the total energy of the perfect crystal in the same supercell. For a charged Cu_M, electrons will be added to or removed from the Fermi level (ε_F), which is conventionally referenced to the valence-band maximum (VBM, E_v) of the host material. An M atom is removed from the supercell and placed in a reservoir with energy μ_M, referenced to the total energy per atom of the metal M ($\mu_M = \tilde{\mu}_M + E_{tot}[M]$), and a Cu atom is taken from a reservoir with energy μ_{Cu}, referenced to the total energy per atom of Cu bulk ($\mu_{Cu} = \tilde{\mu}_{Cu} + E_{tot}[Cu]$). The chemical potentials $\tilde{\mu}_i$ (i = Cu, M, O, H) can be varied and properly adjusted to represent the experimental growth conditions and annealing. The scheme proposed by Freysoldt *et al.*. was used to correct the effects of the finite size of the supercell containing charged defects, as represented in the last term.[51] The static dielectric constants used in the correction were taken from Ref. 23, where the HSE functional with the same fraction HF exchange of 25% was used. Note that this correction scheme for the supercell finite-size yields very similar correction energies as the one proposed by Kumagai and Oba.[52] The approach described above was used to determine the formation energies of the other point defects and H-related complexes in the different charge states.

In thermodynamic equilibrium, the stability condition of $\tilde{\mu}_{Cu} + \tilde{\mu}_M + 2\tilde{\mu}_O = \Delta H_f(CuMO_2)$ must be satisfied, where $\Delta H_f(CuMO_2)$ is the enthalpy of formation of $CuMO_2$, listed in Table I. The calculated $\Delta H_f(CuMO_2)$ values are in good agreement with the experimental values for $CuMO_2$ estimated by Hess's law, i.e., the total enthalpy change of the overall reaction can be estimated as a summation of enthalpy changes of sub-individual reactions, for instance, $\Delta H_f(CuAlO_2) = \left[\Delta H_f(Cu_2O) + \Delta H_f(Al_2O_3)\right]/2$, where $\Delta H_f(Cu_2O)$ and $\Delta H_f(Al_2O_3)$ are the formation enthalpy of Cu_2O and Al_2O_3, respectively. To avoid the formation of the secondary phases, additional bounds were imposed to $\tilde{\mu}_{Cu}$, $\tilde{\mu}_M$, and $\tilde{\mu}_O$; for example, $2\tilde{\mu}_{Al} + 3\tilde{\mu}_O < \Delta H_f(Al_2O_3)$ and $2\tilde{\mu}_{Cu} + \tilde{\mu}_O < \Delta H_f(Cu_2O)$ were included to represent the formation of Cu_2O and Al_2O_3 during equilibrium growth of $CuAlO_2$. We adopted similar procedures to determine the limits in the chemical potentials in the case of $CuGaO_2$ and $CuInO_2$; In ternary metal oxides, these procedures have been widely used to identify stable growth conditions.[53,54] The thermodynamic equilibrium chemical potential diagrams of $CuMO_2$ are shown in Fig. S1 in the supplementary material, are consistent with the diagram in Ref. 23. We chose the O-rich and O-poor conditions to represent the results for the formation energies of the point defects and hydrogen impurities. The chemical potentials ($\tilde{\mu}_{Cu}, \tilde{\mu}_M, \tilde{\mu}_O$) associated with these two conditions are listed in Table II. Note that delafossites $CuMO_2$ are commonly synthesized via solid-state reactions, followed by the fabrication of thin films using pulsed laser deposition (PLD). The preparation process entails annealing the materials at 700 °C, with the O_2 pressure typically ranging from around 10^{-5} to 10^{-4} atm.[8,10] These conditions yield an oxygen chemical potential of about −1.4 eV, aligned with the intermediate condition between the O-rich and O-poor limits.[55] Under both the O-rich and O-poor conditions, the chemical potential of hydrogen, $\tilde{\mu}_H$, is limited by the formation of H_2O, i.e., $\tilde{\mu}_H = \left[\Delta H_f(H_2O) - \tilde{\mu}_O\right]/2$. The calculation of thermodynamic transition levels was conducted using the standard procedure described elsewhere.[4,56]

III. RESULTS AND DISCUSSION

The calculated lattice parameters, direct and indirect bandgaps, and formation enthalpies of $CuAlO_2$, $CuGaO_2$, and $CuInO_2$ are listed in Table I. The calculated and experimental values are in good agreement. Our results for lattice parameters and band gaps of these oxides are consistent with the previously reported values.[23] The range of the Fermi levels in the formation energies corresponds to the calculated fundamental indirect bandgaps.

A. Isolated hydrogen impurities

In our study focusing on the passivation of acceptor defects in delafossite $CuMO_2$, we first investigate the specific hydrogen impurity functioning as a donor. To achieve this, we explore the stability of various possible H impurity configurations within $CuGaO_2$. Given the close similarities in chemical composition and crystal structure of $CuGaO_2$, $CuAlO_2$, and $CuInO_2$, it is assumed that the energetics and electrical characteristics of hydrogen impurities in these materials are also similar. Figure 1 shows the formation energies of possible configurations of H impurities in $CuGaO_2$, including interstitial H adjacent to three Cu atoms (H_i-Cu), bond center (H_i-bc), and antibonding (H_i-ab) as well as the substitutional H at the O site (H_O) for Cu-poor/O-rich and Cu-rich/O-poor conditions. The three possible charge states, −, neutral, and +, for each configuration of H_i were calculated. We find that H_i-ab is stable in the + charge state for the entire range of the Fermi level, thus acting as a shallow donor. In $CuGaO_2$, H_i^+ prefers binding with an O atom, forming a single O–H bond with an O–H bond length of 0.99 Å, as shown in Fig. 1(c). This behavior is similar to other metal oxides such as ZnO, SnO_2, and In_2O_3, in which H_i^+ prefers a site close to the O atom.[25,27,36] We find that H_i is stable in the

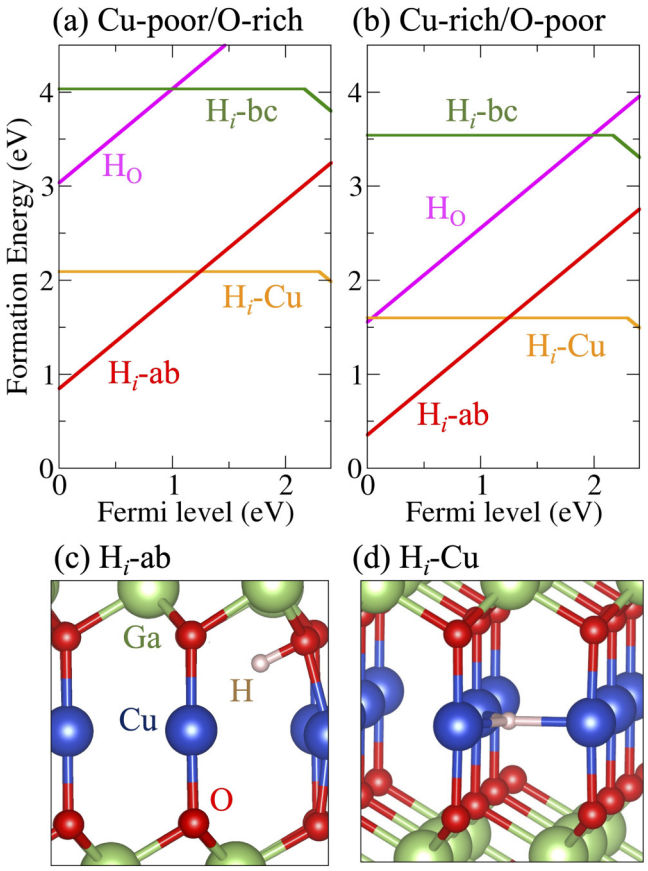

FIG. 1. Formation energies for the H impurities in $CuGaO_2$ as a function of Fermi level under (a) Cu-poor/O-rich and (b) Cu-rich/O-poor limit conditions. The local atomic structure of (c) H_i-ab and (d) H_i-Cu in $CuGaO_2$ are also shown. The local atomic structures of H_O and H_i-bc are shown in Fig. S2 in the supplementary material.

neutral and negative charge states when it is surrounded by three Cu atoms (H_i-Cu) with the Cu–H bond length of 1.69 Å [Fig. 1(d)]. The stability of H_i^- and H_i^0 has been studied in many metal oxides in which the neutral and anionic H_i usually prefer to sit near the cations.[27,57]

Figure 1 shows that neutral H_i-Cu becomes energetically favorable for the Fermi-level positions higher than 1.24 eV. The (0/−) transition level of 0.11 eV below the conduction band indicates that negatively charged H_i-Cu is stable in n-type $CuGaO_2$. In addition, we find that H_i-bc, in which the H atom is located between the Cu and O atoms forming an O–H bond, can be stabilized only in the neutral and negative charge states. However, it has a high formation energy and is, thus, unlikely to be present in the material. For H_O, we find that it is stable exclusively in the positive charge state, acting as a shallow donor. However, its formation is higher than that of interstitial hydrogen, even in the O-poor condition [Fig. 1(b)], likely due to the cost of removing an O atom, as in the formation energy of oxygen vacancy (V_O) in Ref. 23. Therefore, we rule out H_O^+ as a relevant source of compensation for acceptor defects. Our results for H impurities in $CuGaO_2$ are consistent with the generally observed behavior of H in oxides.[36,37] Our calculations show that H_i (H_i-ab) also acts as a shallow donor in $CuAlO_2$ and $CuInO_2$, forming an O–H bond with an O atom (Fig. 2). It is thus reasonable to expect that H_i-ab, behaving as a shallow donor, will likely bind with the dominant acceptors in these materials, forming complex defects that reduce p-type conductivity. The calculated formation energies of other hydrogen impurities in $CuAlO_2$ and $CuInO_2$, shown in Fig. S3 in the supplementary material, confirm that the energetics and electrical characteristics of the hydrogen impurities are similar.

B. Hydrogen-acceptor complexes

The dominant acceptors identified in $CuMO_2$ are Cu_M and V_{Cu}, to which the observed p-type conductivity has been attributed.[22,23] We thus focus on only these acceptors, and our calculations also reveal that these defects are most likely the acceptors present in the samples. Figure 2 shows the calculated formation energies for the antisites, copper vacancies, and H-related complexes in the Cu-poor/O-rich condition, the most energetically favorable condition for the Cu vacancy and the antisite defects. We find that both V_{Cu} and Cu_M act as single acceptors in $CuMO_2$. The transition levels (0/−) of V_{Cu} are at 0.35, 0.37, and 0.35 eV above the respective VBMs for $CuAlO_2$, $CuGaO_2$, and $CuInO_2$. These values are consistent with those reported in Ref. 23. Note that these ionization energies are relatively high, indicating V_{Cu} that the Cu vacancy concentrations will be significantly higher than the hole concentrations. In $CuAlO_2$ and $CuGaO_2$, Cu_{Al} and Cu_{Ga} behave as deep acceptors with the transition levels (0/−) at 0.70 and 0.49 eV, respectively, making them less efficient to generate holes than V_{Cu}. In the case of $CuInO_2$, Cu_{In} can exist in +, neutral, and − charge states, making it an amphoteric defect. The transition levels (+/0) and (0/−) for Cu_{In} are at 0.10 and 0.34 eV, respectively. In this case, Cu_{In} and V_{Cu} are equally capable of producing holes, with equal ionization energies. The results shown in Fig. 2, therefore, indicate that V_{Cu} is the likely although rather inefficient source of hole conductivity in $CuAlO_2$ and $CuGaO_2$, while in $CuInO_2$, both Cu_{In} and V_{Cu} could be responsible for *p*-type conductivity (also rather inefficiently due to the high ionization energy).

Isolated H_i^+ are highly mobile species in several metal oxides, such as SnO_2, $SrTiO_3$, and Cu_2O, with calculated migration barriers of 0.57,[36] 0.25,[58] and 0.18 eV,[35] respectively. Therefore, H_i^+ are likely to form complexes with acceptors due to Coulomb attraction. We investigated the plausible configurations for the H-acceptor complexes, i.e., (1) H_i−Cu_M, (2) H_i-V_{Cu}, and (3) $2H_i$-V_{Cu}, which are shown in Fig. 3. For the H_i–Cu_M complexes, H prefers to bond to an O atom adjacent to acceptor Cu_M. The Cu–O bond length is elongated by 23%–28% (Fig. 3) compared to the equilibrium Cu–O bond length in the supercell with isolated Cu_M. The Cu–H distances are 1.86, 1.90, and 2.00 Å in $CuAlO_2$, $CuGaO_2$, and $CuInO_2$, respectively. As shown in Fig. 2, the H_i−Cu_M complexes are exclusively stable in the neutral charge state, except in $CuAlO_2$, where the complex is also stable in the positive charge state at Fermi-level positions close to the VBM. The formation energies of H_i−Cu_{Ga} and H_i−Cu_{Al} complexes are relatively high, around 1 eV, which is

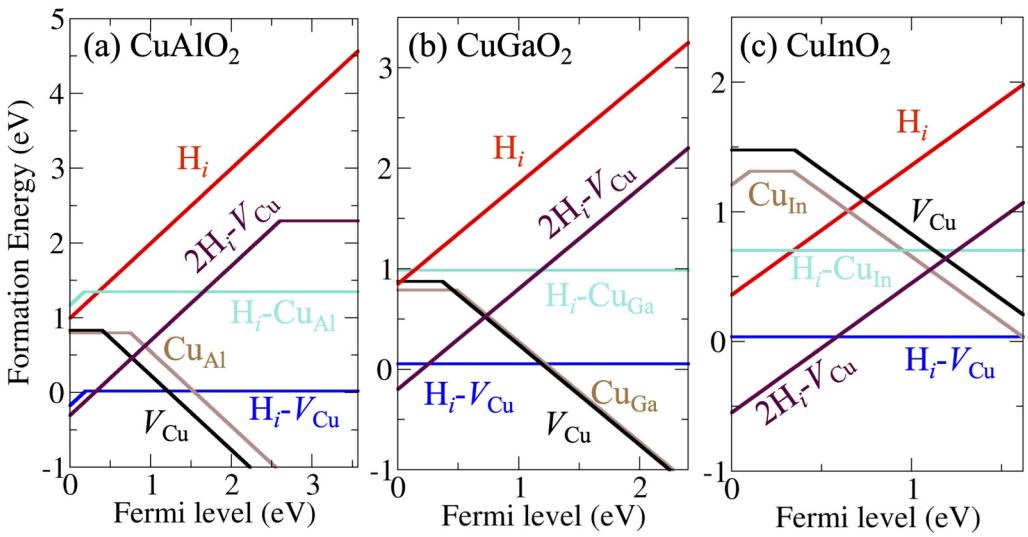

FIG. 2. Formation energies for the H impurity and the H-acceptor complexes, including the donor H_i, copper vacancy V_{Cu}, and copper antisite Cu_M as a function of Fermi level in (a) $CuAlO_2$, (b) $CuGaO_2$, and (c) $CuInO_2$, in the Cu-poor/O-rich condition.

higher than Cu_M in $CuAlO_2$ and $CuGaO_2$ for all Fermi-level positions. This suggests these complexes will not be present at high concentrations. However, they can partially passivate the Cu_{Ga} and Cu_{Al} acceptors. The H_i-Cu_{In} complex in $CuInO_2$ has reasonably low formation energy, which is lower than Cu_{In} for Fermi-level positions up to 1 eV, indicating that it should be easily formed and passivate Cu_{In} in p-type $CuInO_2$. In the case of the H_i-V_{Cu} complexes, interstitial H tends to bond with an adjacent O atom to V_{Cu} in all three materials. In the presence of V_{Cu} next to H_i-ab, the H atom tends to relax and point toward the vacancy, as illustrated in Fig. 3. It is worth noting that H_i–V_{Cu} complexes are stable only in the neutral charge state in $CuGaO_2$ and $CuInO_2$, while it is stable in the positive charge state when the Fermi level is close to the VBM in $CuAlO_2$ with (+/0) transition level ~0.1 eV. Due to their significantly lower formation energies, which are more than 1 eV lower than H_i–Cu_M complexes, as depicted in Fig. 2, they are expected to form in much higher concentrations. Once formed, these complexes tend to be highly stable and can act as passivation centers for acceptors, leading to a reduction in hole carriers.

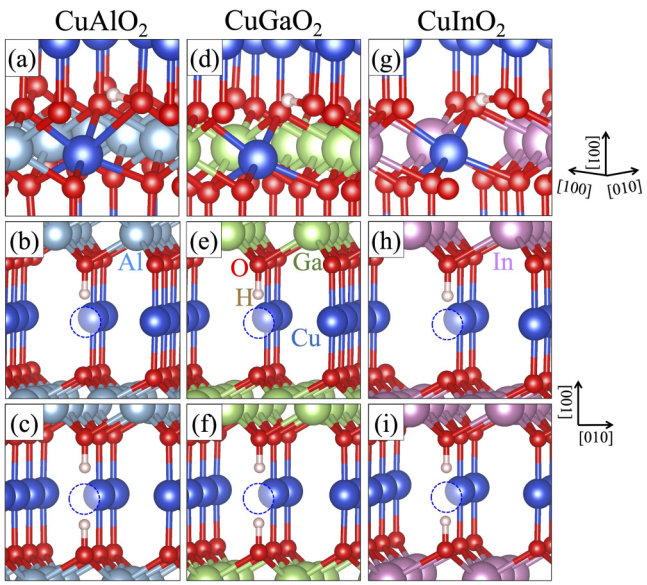

FIG. 3. Local atomic structures of H_i–Cu_M, H_i–V_{Cu}, and $2H_i$–V_{Cu} in $CuAlO_2$ [(a)–(c)], $CuGaO_2$ [(d), (e), and (f)], and $CuInO_2$ [(g), (h), and (i)]. The dashed circles represent the locations of the missing copper atoms (Cu vacancies).

Our results suggest that both types of complexes H_i–Cu_M and H_i–V_{Cu} take part in the passivation of the acceptors. To reactivate the acceptors, the H atom in these complexes would have to overcome the energy required to dissociate a defect complex. The activation energy for the dissociation can be estimated by the sum of the binding energy of the complex and migration barrier of interstitial H.[59] The binding energy of H_i-Cu_M in charge state q is given by

$$E_b[(H_i - Cu_M)^q] = E^f\left[H_i^+\right] + E^f\left[Cu_M^{q'}\right] - E^f[(H_i - Cu_M)^q], \quad (2)$$

where $E^f[(H_i - Cu_M)^q]$ is the formation energy of the H_i–Cu_M complex in charge state q ($q = 0, +$), $E^f[H_i^+]$ is the formation energy of isolated H_i^+ and $E^f\left[Cu_M^{q'}\right]$ is the formation energy of isolated Cu_M in charge state q' ($q' = +, 0, -$). A positive binding energy indicates that the H_i and Cu_M tend to bind together,

forming a stable complex. Although a positive E_b indicates the potential formation of a complex, it does not guarantee the formation. The concentration of the complex will be low if E_b is not large enough compared to the formation energy of the parent defects. This is because the configuration entropy of the complex is much smaller. The calculated binding energy of H_i–Cu_M as a function of Fermi level is shown in Fig. 4. The binding energies range from 1.1 to 1.3 eV for most Fermi-level positions but decrease to 0.6–0.9 eV for the Fermi-level positions close to the VBM (p-type). These values are comparable to H_i-acceptor complexes in other oxides, such as H_i–Al_{Sn} and H_i–Ga_{Sn} in SnO_2.[59] However, the values in $CuMO_2$ are slightly larger, possibly due to shorter H_i-acceptor distances. Given the magnitude of binding energies in these ranges, which are not much larger than the formation energies of H_i and Cu_M, for Fermi level near the VBM, the concentration of H_i–Cu_M complex will be low. For the H_i–V_{Cu} complex, the binding energy also can be calculated by adopting the same procedure. Our calculations show that the binding energies of the H_i–V_{Cu} complexes are 2.0–2.2 eV for most of the Fermi-level positions in all materials. Magnitude of the binding energies are comparable to the H_i–V_{Cu} complexes in semiconducting oxides.[32,33] These much higher binding energies than those of the H_i–Cu_M complexes are due to the very low formation energies of the H_i–V_{Cu} complexes. Figure 2 shows that the formation energies of the $H_i - V_{Cu}$ complexes are always lower than H_i^+, suggesting that incorporated H are unstable in the form of isolated interstitials. They would bind with V_{Cu} into stable H_i-V_{Cu} complexes, likely formed in high concentrations.

In addition, we find that the second H can enter the H_i–V_{Cu} complex by bonding with another O atom next to V_{Cu} into $2H_i$–V_{Cu}, as shown in Figs. 3(c), 3(f), and 3(i). According to our calculations, the H_i–V_{Cu} complex is mostly stable in the neutral charge state. However, if an extra H is present, $2H_i$-V_{Cu} is expected to occur in the positive charge state. Our results, depicted in Fig. 2, show that $2H_i$–V_{Cu} complexes behave as donors in $CuMO_2$, and

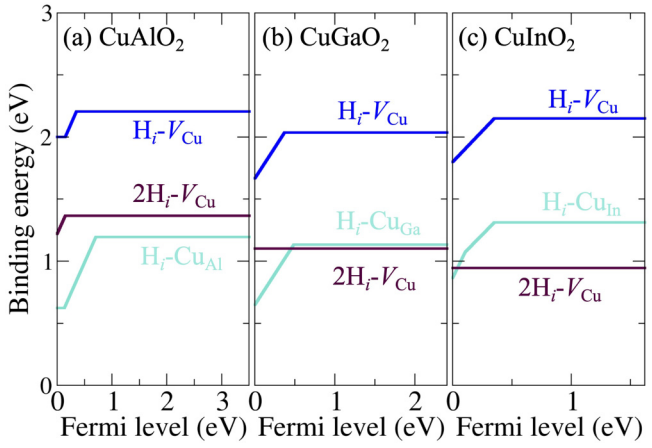

FIG. 4. Binding energies of H_i-V_{Cu}, H_i-V_{Cu}, and $2H_i$–V_{Cu} complexes in (a) $CuAlO_2$, (b) $CuGaO_2$, and (c) $CuInO_2$ as a function of the Fermi level.

are always lower in energy than H_i^+ in all materials. The complex acts as a deep donor in $CuAlO_2$ and a shallow donor in $CuGaO_2$ and $CuInO_2$ and could act as a hole killer in p-type $CuMO_2$. The binding energy of $2H_i$-V_{Cu} for dissociating into H_i^+ and $(H_i{-}V_{Cu})^0$ is large and positive, as shown in Fig. 4. We also consider the possibility of molecular hydrogen, H_2 being trapped at the Cu vacancy in the form of H_2–V_{Cu} complex. The complex is stable in the negative charge state since it comprises a neutral H_2 and a V_{Cu}^-. We find that $(H_2{-}V_{Cu})^-$ has much higher formation energy than $(2H_i{-}V_{Cu})^+$ in p-type $CuAlO_2$ and $CuGaO_2$ but has lower formation energy under n-type conditions. In $CuInO_2$, however, $(H_2{-}V_{Cu})^-$ is never thermodynamically stable compared to $(2H_i{-}V_{Cu})^+$. It is unlikely that the H_2–V_{Cu} complex will form easily against the $2H_i$-V_{Cu} because the Cu vacancy is surrounded by reactive O dangling bonds that will readily react with H atoms. Hydrogenated cation vacancies have been investigated in several n-type TCOs such as SnO_2, In_2O_3, Ga_2O_3, and $SrTiO_3$, where the binding energies of the H_i–cation vacancy complexes in these oxides, except for $SrTiO_3$, are more prominent than in $CuMO_2$.[32,33]

Our calculations of H_i migration based on the nudged elastic band method show that H_i^+ are very mobile with the migration barriers of 0.40, 0.52, and 0.54 eV in $CuAlO_2$, $CuGaO_2$, and $CuInO_2$, respectively. Combined with the calculated binding energies, the activation energy E_a to dissociate the H_i-Cu_M complexes into isolated H_i^+ and Cu_{M^-} are 1.6–1.8 eV. The dissociation temperature, T, can be estimated with transition state theory in which a defect hops to a neighboring site with the rate $\Gamma = \Gamma_0 \exp\left(-\frac{E_a}{k_B T}\right)$, where k_B is the Boltzmann constant. The prefactor Γ_0 can be approximated by the optical phonon frequency in $CuMO_2$, i.e., 10^{12} Hz.[60] We estimate the dissociation temperature as the temperature at which the complex starts dissociating with the rate $\Gamma = 1\,s^{-1}$. The dissociation temperature, however, is not very sensitive to the choice of Γ_0. Using this estimation, the dissociation temperatures of the H_i–Cu_M complexes are around 300–400 °C. For the H_i–V_{Cu} complexes, the estimated activation energies are 2.5–2.7 eV, indicating much higher dissociation temperatures. Using analogous estimation, we obtain the dissociation temperatures of 600–700 °C. These suggest that post-annealing at high temperatures up to 700 °C is required to dissociate the H_i-V_{Cu} and $2H_i$-V_{Cu} complexes. At these high temperatures, interstitial H would diffuse out due to its low migration barrier. Even though there have never been reported for the migration barriers of V_{Cu}^- in delafossite $CuMO_2$, it is expected that V_{Cu}^- would readily diffuse out, given that the out-diffusion temperature of cation vacancies in other oxides ranges from 250 to 400 ° C.[4,32] At these temperatures, Cu_{M^-} is expected to be immobile due to the high migration energy barrier. To migrate, the defect must split into Cu_i and V_M constituents, which involves breaking six Cu–O bonds. This process will likely be very difficult due to a high migration barrier. Therefore, Cu_{M^-} generally remains fixed in its position, while other defects may migrate more easily under the same conditions. This indicates that Cu_{M^-} would be dominant acceptors after post-annealing in $CuMO_2$. Furthermore, our findings suggest that by manipulating hydrogen concentrations through various processing techniques,

we can potentially optimize the p-type conductivity in these materials and unlock their full potential for diverse electronic applications.

IV. CONCLUSIONS

Our hybrid-functional calculations reveal the crucial role of hydrogen in governing the p-type conductivity of delafossite $CuMO_2$ (M = Al, Ga, In) oxides. We find that hydrogen acts as a shallow donor and readily forms stable, electrically inactive complexes with copper vacancies (H_i-V_{Cu}). These complexes, characterized by significant binding energies, are prevalent under growth conditions. Additionally, hydrogen can form $2H_i$–V_{Cu} complexes that act as single donors. Both H_i-V_{Cu} and $2H_i$-V_{Cu} are likely dissociated at temperatures between 600 and 700 °C, releasing hydrogen and copper vacancies, which are likely diffused out. Conversely, hydrogen can bind to antisite defects (H_i–Cu_M), but these complexes exhibit lower binding energies and potentially dissociate into isolated H_i and Cu_M at 300–400 °C. Our work suggests that, at low post-annealing temperatures, Cu_M defects become reactivated and dominate p-type conductivity in these oxides.

SUPPLEMENTARY MATERIAL

See the supplementary material for the calculated thermodynamic chemical potential diagrams of delafossite $CuGaO_2$, $CuAlO_2$, and $CuInO_2$; the atomic configurations of H_i-bc and H_O; and the formation energies of isolated hydrogen impurities in $CuGaO_2$, $CuAlO_2$, and $CuInO_2$.

ACKNOWLEDGMENTS

This work was supported by the Thailand Research Fund (Grant No. RSA6280068). P.R. acknowledged support from Kasetsart University Research and Development Institute (FF(KU) 28.67). S.J. acknowledges funding support from the NSRF via the Program Management Unit for Human Resources and Institutional Development, Research, and Innovation (Grant No. B39G670018). I.C. acknowledges support from Development and Promotion of Science and Technology Talents Project (DPST) administered by the Institute for the Promotion of Teaching Science and Technology (IPST), Thailand. We thank the NSTDA Supercomputer Center (ThaiSC) for providing computing resources for this work.

AUTHOR DECLARATIONS

Conflict of Interest

The authors have no conflicts to disclose.

Author Contributions

Aroon Ananchuensook: Data curation (equal); Investigation (lead); Writing – original draft (equal). **Intuon Chatratin:** Investigation (supporting); Writing – review & editing (supporting). **Anderson Janotti:** Supervision (equal); Writing – review & editing (equal). **Teeraphat Watcharatharapong:** Resources (supporting); Writing – review & editing (supporting). **Jiraroj T-Thienprasert:** Software (supporting); Writing – review & editing (supporting). **Adisak Boonchun:** Software (supporting); Writing – review & editing (supporting). **Sirichok Jungthawan:** Funding acquisition (supporting); Writing – review & editing (supporting). **Pakpoom Reunchan:** Conceptualization (lead); Investigation (equal); Supervision (lead); Writing – review & editing (lead).

DATA AVAILABILITY

The data that support the findings of this study are available from the corresponding author upon reasonable request.

REFERENCES

[1]K. Ellmer, Nat. Photonics **6**, 809 (2012).
[2]R. G. Gordon, MRS Bull. **25**, 52 (2000).
[3]A. Boonchun and W. R. L. Lambrecht, Phys. Rev. B **81**, 024103 (2010).
[4]A. Janotti and C. G. Van de Walle, Phys. Rev. B **76**, 165202 (2007).
[5]J. Willis and D. O. Scanlon, J. Mater. Chem. C **9**, 11995 (2021).
[6]K. H. L. Zhang, K. Xi, M. G. Blamire, and R. G. Egdell, J. Phys.: Condens. Matter **28**, 383002 (2016).
[7]H. Hosono, Thin Solid Films **515**, 6000 (2007).
[8]H. Kawazoe, M. Yasukawa, H. Hyodo, M. Kurita, H. Yanagi, and H. Hosono, Nature **389**, 939 (1997).
[9]K. Ueda, T. Hase, H. Yanagi, H. Kawazoe, H. Hosono, H. Ohta, M. Orita, and M. Hirano, J. Appl. Phys. **89**, 1790 (2001).
[10]H. Yanagi, T. Hase, S. Ibuki, K. Ueda, and H. Hosono, Appl. Phys. Lett. **78**, 1583 (2001).
[11]S. A. Mary, B. G. Nair, J. Naduvath, G. S. Okram, S. K. Remillard, P. V. Sreenivasan, and R. R. Philip, J. Alloys Compd. **600**, 159 (2014).
[12]H. F. Jiang, X. B. Zhu, H. C. Lei, G. Li, Z. R. Yang, W. H. Song, J. M. Dai, Y. P. Sun, and Y. K. Fu, Thin Solid Films **519**, 2559 (2011).
[13]B. G. Nair, H. Rahman, V. Sharma, G. S. Okram, U. Deshpande, V. Ganesan, and R. Reena Philip, Mater. Sci. Eng. B **255**, 114520 (2020).
[14]C.-Y. Tsay and C.-L. Chen, Ceram. Int. **43**, 2563 (2017).
[15]A. R. C. Bredar, M. D. Blanchet, R. B. Comes, and B. H. Farnum, ACS Appl. Energy Mater. **2**, 19 (2019).
[16]A. Renaud, B. Chavillon, L. Le Pleux, Y. Pellegrin, E. Blart, M. Boujtita, T. Pauport, L. Cario, S. Jobic, and F. Odobel, J. Mater. Chem. **22**, 14353 (2012).
[17]T. Omata *et al.*, J. Am. Chem. Soc. **136**, 3378 (2014).
[18]J. Tate, H. L. Ju, J. C. Moon, A. Zakutayev, A. P. Richard, J. Russell, and D. H. McIntyre, Phys. Rev. B **80**, 165206 (2009).
[19]X. Nie, S.-H. Wei, and S. B. Zhang, Phys. Rev. Lett. **88**, 066405 (2002).
[20]D. O. Scanlon and G. W. Watson, J. Mater. Chem. **21**, 3655 (2011).
[21]D. O. Scanlon, A. Walsh, B. J. Morgan, G. W. Watson, D. J. Payne, and R. G. Egdell, Phys. Rev. B **79**, 035101 (2009).
[22]D. O. Scanlon and G. W. Watson, J. Phys. Chem. Lett. **1**, 3195 (2010).
[23]T. Gake, Y. Kumagai, A. Takahashi, and F. Oba, Phys. Rev. Mater. **5**, 104602 (2021).
[24]H. Okumura, K. Sato, and T. Kakeshita, J. Appl. Phys. **123**, 161584 (2018).
[25]A. Janotti and C. G. Van de Walle, Nat. Mater **6**, 44 (2007).
[26]E. V. Lavrov, F. Herklotz, and J. Weber, Phys. Rev. B **79**, 165210 (2009).
[27]S. Limpijumnong, P. Reunchan, A. Janotti, and C. G. Van de Walle, Phys. Rev. B **80**, 193202 (2009).
[28]A. K. Singh, A. Janotti, M. Scheffler, and C. G. Van de Walle, Phys. Rev. Lett. **101**, 055502 (2008).
[29]W. M. Hlaing Oo, S. Tabatabaei, M. D. McCluskey, J. B. Varley, A. Janotti, and C. G. Van de Walle, Phys. Rev. B **82**, 193201 (2010).
[30]J. B. Varley, J. R. Weber, A. Janotti, and C. G. Van de Walle, Appl. Phys. Lett. **97**, 142106 (2010).
[31]E. V. Lavrov, J. Weber, F. Börrnert, C. G. Van de Walle, and R. Helbig, Phys. Rev. B **66**, 165205 (2002).

[32]J. B. Varley, H. Peelaers, A. Janotti, and C. G. Van de Walle, J. Phys.: Condens. Matter **23**, 334212 (2011).
[33]J. B. Varley, A. Janotti, and C. G. Van de Walle, Phys. Rev. B **89**, 075202 (2014).
[34]P. Weiser, M. Stavola, W. B. Fowler, Y. Qin, and S. Pearton, Appl. Phys. Lett. **112**, 232104 (2018).
[35]D. O. Scanlon and G. W. Watson, Phys. Rev. Lett. **106**, 186403 (2011).
[36]K. Biswas, M. H. Du, J. T-Thienprasert, S. Limpijumnong, and D. J. Singh, Phys. Rev. Lett. **108**, 219703 (2012).
[37]H. Li and J. Robertson, J. Appl. Phys. **115**, 203708 (2014).
[38]T. Ishiguro, A. Kitazawa, N. Mizutani, and M. Kato, J. Solid State Chem. **40**, 170 (1981).
[39]B. Köhler and M. Jansen, Z. Anorg. Allg. Chem. **543**, 73–80 (1986).
[40]M. Sasaki and M. Shimode, J. Phys. Chem. Solids **64**, 1675 (2003).
[41]J. Pellicer-Porres, A. Segura, A. S. Gilliland, A. Muñoz, P. Rodríguez-Hernández, D. Kim, M. S. Lee, and T. Y. Kim, Appl. Phys. Lett. **88**, 181904 (2006).
[42]J. W. Lekse, M. K. Underwood, J. P. Lewis, and C. Matranga, J. Phys. Chem. C **116**, 1865 (2012).
[43]M. Binnewies and E. Milke, *Thermochemical Data of Elements and Compounds* (Wiley Online Library, 2002), Vol. 168.
[44]W. Kohn and L. J. Sham, Phys. Rev. **140**, A1133 (1965).
[45]J. Heyd, G. E. Scuseria, and M. Ernzerhof, J. Chem. Phys. **118**, 8207 (2003).
[46]J. Heyd, G. E. Scuseria, and M. Ernzerhof, J. Chem. Phys. **124**, 219906 (2006).
[47]G. Kresse and J. Furthmüller, Phys. Rev. B **54**, 11169 (1996).
[48]G. Kresse and J. Furthmüller, Comput. Mater. Sci. **6**, 15 (1996).
[49]P. E. Blöchl, Phys. Rev. B **50**, 17953–17979 (1994).
[50]G. Kresse and D. Joubert, Phys. Rev. B **59**, 1758 (1999).
[51]C. Freysoldt, J. Neugebauer, and C. G. Van de Walle, Phys. Rev. Lett. **102**, 016402 (2009).
[52]Y. Kumagai and F. Oba, Phys. Rev. B **89**, 195205 (2014).
[53]P. Reunchan, N. Umezawa, A. Janotti, J. T-Thienprasert, and S. Limpijumnong, Phys. Rev. B **95**, 205204 (2017).
[54]S. Charoenphon, A. Tubtimtae, I. Watanabe, S. Jungthawan, J. T-Thienprasert, A. Boonchun, and P. Reunchan, Phys. Chem. Chem. Phys. **25**, 19116 (2023).
[55]K. Reuter and M. Scheffler, Phys. Rev. B **65**, 035406 (2001).
[56]I. Chatratin, F. P. Sabino, P. Reunchan, S. Limpijumnong, J. B. Varley, C. G. Van de Walle, and A. Janotti, Phys. Rev. Mater. **3**, 074604 (2019).
[57]C. G. Van de Walle, Phys. Rev. Lett. **85**, 1012 (2000).
[58]J. T-Thienprasert, I. Fongkaew, D. J. Singh, M. H. Du, and S. Limpijumnong, Phys. Rev. B **85**, 125205 (2012).
[59]J. B. Varley, A. Janotti, A. K. Singh, and C. G. Van de Walle, Phys. Rev. B **79**, 245206 (2009).
[60]J. Pellicer-Porres, A. Segura, E. Martínez, A. M. Saitta, A. Polian, J. C. Chervin, and B. Canny, Phys. Rev. B **72**, 064301 (2005).